A 38 GHz Cellular Outage Study for an Urban Outdoor Campus Environment

^James N. Murdock, Eshar Ben-Dor, Yijun Qiao, Jonathan I. Tamir and * Theodore S. Rappaport
^Wireless Networking and Communications Group (WNCG), The University of Texas, Austin, TX 78712
* Wireless Internet Center for Advanced Technologies (WICAT), New York University, 10012
*Email: TSR at NYU dot EDU

***Abstract*— Wireless systems require increasingly large system bandwidths that are only available at millimeter-wave frequencies. Such spectrum bands offer the potential for multi-gigabit-per-second data rates to low-cost *massively broadband*® devices. To enable mobile outdoor millimeter-wave cellular-type applications, it is necessary to determine the coverage potential of base stations in real-world environments. This paper presents the results of a measurement campaign of 38 GHz outdoor urban cellular channels using directional antennas at both the mobile and the base station, and assesses outage probabilities at two separate transmitter locations on the campus of The University of Texas at Austin. Our measurements demonstrate the viability of directional antennas and site-specific planning for future mm-wave cellular, and show that cell radii of ~ 200 m will provide a very high probability of coverage in an urban environment. As production costs for millimeter-wave technologies continue to fall [1], we envision millimeter-wave cellular systems with dense base station deployments as a cost effective means of delivering multi-Gbps data rates to mobile cell phone and internet users.**

Keywords – RF propagation measurements, channel sounding; Millimeter Wave Communications; site-specific

I. INTRODUCTION

Wireless systems, from cellular networks to short-range 60 GHz ad hoc WPANs (Wireless Personal Area Networks), are moving rapidly to accommodate greater bandwidths for multi-Giga-bit-per-second data rates [1]. Consequently, communication systems that use carrier frequencies in the millimeter-wave range – an order of magnitude higher in the radio spectrum than carrier frequencies used in today's cellular networks – will become ubiquitous [1]. Providing mobile users with multi-Gpbs wireless services motivates our investigation of millimeter-wave outdoor and indoor cellular systems, in which an elevated base station communicates with receivers near ground level. At mm-wave frequencies, the wavelength is an order of magnitude smaller than today's cellular frequencies, allowing for the use of much smaller and steerable high gain antennas on handsets. An open question for futuristic mm-wave mobile systems is whether or not radio propagation will support such systems in dense outdoor urban settings. Earlier studies of 28 GHz fixed LMDS systems showed that NLOS (non-line-of-sight) paths exist and can be used to increase coverage, but that they are highly dependent on the receiver's local environment [2] [3]. These previous studies, in which the receiver is fixed and elevated at least 3 m above ground (in contrast to cellular systems where the receiver is mobile and at head or hand level), suggested that only areas covered by LOS (line-of-sight) paths from the base station to the receiver can reliably provide sufficiently strong received signal powers [3]. As costs continue to decrease for millimeter-wave CMOS technology, beamforming antennas, and MIMO diversity techniques, mm-wave microcell infrastructure will soon be practical [1], [4]. To assess the viability of futuristic mm-wave mobile systems, we performed a 38 GHz millimeter-wave channel measurement campaign that was designed to assess the coverage and outage probabilities of two typical base station locations at The University of Texas at Austin campus. The base stations are located in an urban campus with closely spaced buildings and light to medium tree cover.

In [5], [6], and [7], we presented propagation studies for 38 and 60 GHz outdoor urban channels for both peer-to-peer and cellular applications using steerable, highly directional 7^{o} beamwidth transmit and receive antennas, as well as wider beamwidth 50^{o} antennas for the receiver mobile antenna. Our measurements focused on ranges up to 1 km for outdoor cellular channels. We found that LOS links at both 38 and 60 GHz are comparable to free-space, while obstructed paths have a path loss exponent of 3.26 when the single strongest NLOS beamformed link is considered at each of the receiver locations, and 3.88 when all of the different viable antenna pointing links are considered across all receiver locations. We found that the RMS delay spread for the outdoor cellular channel with directional antennas is less than 225 ns and that the RMS delay spread distribution for narrow and wide beam receiver antennas are highly similar. In [5]-[7], we studied the characteristics of links that can be formed (e.g links conditioned on not being in an outage), but we did not consider outage over a wide range of blindly selected obstructed mobile locations.

References [8]-[11] provide analytical methods for determining outage probability in traditional wireless systems. Traditional outage assessments rely on statistical models for shadowing and assume circular cell shapes. However, as we show here, for mm-wave urban cell diameters on the order of a kilometer or less, the diffraction propagation mechanism is much weaker than experienced at today's low cellular frequencies. Thus, propagation will be primarily due to direct LOS or reflected paths, and traditional shadowing caused by the diffraction mechanism will have much less impact than in today's mobile systems.

Studies of traditional cellular/microcell systems [8]-[11] show the importance of path loss variation caused by shadowing, since as the statistical deviation of path loss increases, the probability of outage also increases. Our results show that at 38 GHz, outages caused by shadowing occur in identifiable clusters due to buildings, thus pointing to the viability of site-specific placement of infrastructure to predict coverage and outage [12], [13]. Here, we devise a blind test to select random outdoor cellular measurement locations and use a reasonable commercial link budget. We found that at 38 GHz, transmitter-receiver (T-R) separation distances of ~ 200 m provide a very high probability of link establishment, as long as steerable beamforming is used at the base station and mobile. This implies that traditional statistical outage analysis approaches may still be valid as long as the T-R separation is small enough to greatly reduce the likelihood of outage. These smaller mm-wave cell sites will also be needed to allow for sufficient link margin for rain and hail variations [1], [6].

Today, the problems of outage and intercell interference plague dense heterogeneous network deployments of current cellular technologies, but these problems would be greatly reduced with the use of highly directional steerable beam antenna arrays at the mobile devices and base stations. As illustrated in Fig. 1, nearby interferers are unlikely to be incident on the boresight direction of the mobile's antenna. Therefore, millimeter-wave cellular systems with small, yet directional, beamforming antennas at both the handset and base station will be primarily noise limited, rather than interference limited. Such insight, combined with the likely dominance of site-specific planning for the infrastructure placement of these systems [12],[13] has motivated our current work to focus on received signal power and outage, rather than intercell interference analysis (which will eventually be required for commercial deployment).

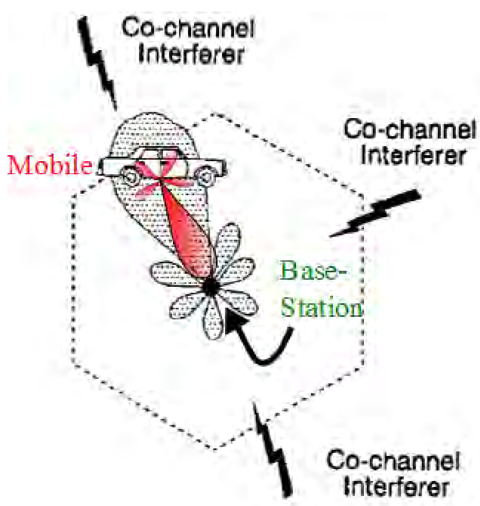

Figure 1. Highly directional receiver antennas in cellular millimeter-wave systems would significantly reduce interference due to the attenuation caused by the antenna beam-pattern off-boresight. Figure adapted from [14].

Analytic or statistical outage models require measured channel data for development and validation. In [15], 28 GHz propagation measurement data in a suburban environment with a 2 km radius found coverage likelihoods of 60% and 80% for a receiver height of 40 ft and 80 ft, respectively. In [16], reflection characteristics at 42 GHz were observed, and showed the potential for NLOS links in millimeter-wave systems due to reflections. Work in [17] estimated rain attenuation at 7.5 dB/km for fixed LMDS systems, and discussed the potential for NLOS paths to increase coverage to areas without direct LOS paths to the transmitter. Papers [2], [3], and [10] studied the impact of transmitter and receiver height on coverage. These early works occurred well before today's CMOS revolution, and before the tremendous demand for massive bandwidths brought about from the explosion of smart phones and cloud computing [1].

The paper is organized as follows: In Section II we describe the measurement hardware used in the measurement campaign. Section III describes the experimental design, including the use of blind, randomly selected receiver locations to ensure accurate conclusions about outage probability. Section IV presents the measurement results and analysis, and conclusions are discussed in Section V.

II. MEASUREMENT HARDWARE

A sliding correlator channel sounder [18], first proposed for cellular channel measurements in [19], was constructed for this outage study. Our sliding correlator transmitter uses an 11-bit pseudonoise (PN) sequence clocked at 400 MHz, yielding an 800 MHz first zero-crossing RF bandwidth signal. The PN signal is upconverted to a 37.625 GHz carrier as shown in [6] with output power of +21.2 dBm. A 25dBi vertically-polarized steerable horn antenna with a beamwidth of 7.0^{o} is used to provide a highly directional broadband sounding signal with EIRP of +46.2 dBm, on the order of today's micro- cellular base stations.

The receiver uses a superheterodyne downconversion chain that uses a 5.375 GHz IF and performs quadrature demodulation where both in-phase and quadrature components of the received signal are multiplied by an identical 11-bit PN sequence which is clocked at the slightly slower rate of 399.95 MHz. The resulting waveforms are low-pass filtered to generate a time-dilated (i.e. frequency compressed) representation of the PN autocorrelation [6], [18]. A power delay profile is generated by adding the squares of the in-phase and quadrature parts. The received power is determined through integration of the PDP after noise is removed through a thresholding operation. Multipath energy is then summed to determine total received power. In practice, multipath links will be exploited to increase SNR in mm-wave cellular systems using signal processing and/or antenna/RF combining (depending on symbol rates and handset cost and power consumption constraints).

III. EXPERIMENTAL DESIGN

Two transmitter locations on the rooftops of adjacent buildings on The University of Texas at Austin campus were used for this study. At each location, the transmitter antenna was placed on a tripod at a height of 1.5 m above the roof of each building, positioned in the middle of each roof's western edge (to avoid shadowing by the roof directly in front of the antenna). This imitated a typical sector-antenna installation used in today's microcell deployments, where base station antennas are mounted on the external wall or edge of a multi-story building, rather than the older macrocellular towers that uses a tall mast. The microcell approach allows for dense base station deployments in urban settings, and uses surrounding buildings to reduce inter-cell interference by containing the coverage in specific sectors. The first transmitter location was on the roof of the Engineering Science Building (ENS) at a height of 36 m (8 stories) above ground. The second transmitter location was on the roof of nearby W.R. Woolrich Laboratories (WRW) at a height of 18 m (4 stories) above ground. The significant height difference was chosen to evaluate how the outage probability varies as a function of transmitter height in the same campus region.

The investigated region lies within the university campus and represents an urban area with short walking distances between densely packed multi-story buildings, a large number of vehicles and trees, and active construction zones. Fig. 2 displays the distribution of buildings in the 460 m x 740 m measurement region. The overlaid topographic contours indicate a total of 55 feet of elevation variation over the entire study area. Construction zones are shaded in yellow. Metallic construction cranes of approximately 50 m height were present in the zone labeled DCS. Buildings are indicated by three-letter initials.

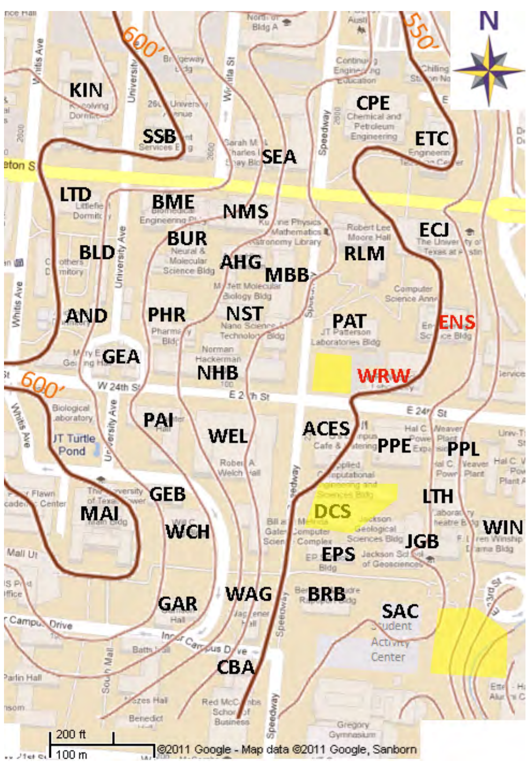

Figure 2. A 460 m x 740 m map showing the investigated region of the The University of Texas at Austin. Topographic contours show the increase in elevation in the western direction. Construction zones are shaded in yellow.

For each of the two base station transmitter locations, the same set of receiver locations were tested for outage. In order to ensure random selection of receiver locations, a contiguous grid of 20 m x 20 m squares was drawn over the 460 m by 740 m site map of Fig. 2 (not shown). The grid consisted of 23 grid squares in the east-west direction and 37 grid squares in the north-south direction. A random number generator was used to blindly select measurement grid locations at random. Then, the selected grid squares were examined to determine which squares lay completely outside of buildings and which were accessible to our measurement equipment and researchers. The resulting 53 randomly selected receiver location grid squares represent 6.2% of the total considered measurement area. Using the grid square approach, we observed that approximately 50% of the grid squares were partially or fully contained within campus buildings. Thus, the selected blind measurement locations represent approximately 12.4% of the total available outdoor measurements in the campus area shown in Fig. 2.

For each of the 53 receiver locations, the directional antennas at the receiver and transmitter were exhaustively scanned in both azimuth and elevation angular directions to search for the presence of a received signal above the system sensitivity of 160 dB path loss at 800 MHz RF bandwidth [6]. Since our sliding correlator has better (lower) noise figure and enhanced processing gain compared to eventual commercial mm-wave systems, we also determined outages at each receiver location using a 10 dB smaller (e.g. 150 dB) path loss threshold to determine outage probability for lower system sensitivity or smaller link budgets.

IV. Measurement Results and Analysis

All receiver locations were within 500 m of both transmitter locations. Figs. 3 and 4 show the transmitter locations with an orange star. The 53 receiver locations are marked with circular dots. The color of each circle indicates whether a link below 150 dB path loss was made (green dot), whether an outage (lack of any detectable signal) occurred (red), or if there was a detectable link between 150 and 160 dB path loss (yellow). The shaded regions on Figs. 3 and 4 show locations that offered an optical line of sight (LOS) from the transmitter. As expected, all receiver locations with a clear LOS, and those locations only obstructed by foliage, produced strong links (e.g. green dots). More surprisingly, links were also made at most of the obstructed locations within 400 m of the ENS transmitter (Fig. 3). As shown in Table I, for the tall ENS base station, only 18.9% of all 53 receiver locations resulted in outage based on a system sensitivity of 160 dB maximum path loss. Notably, *all locations* within 200 m of the transmitter received a signal with less than 160 dB path loss (e.g. 0% outage). However, certain locations within a 200 m radius were sufficiently obstructed to produce a weak signal (more than 150 dB but less than 160 dB path loss). The number of these weaker receiver locations is significant enough that the lower sensitivity system (150 dB path loss) would experience an outage at 27.3% within a 200 m radius of the ENS transmitter location, even with directional steerable antennas at both base and mobile. The outage rate for >160 dB path loss increases to 52.8% when receiver locations beyond a 200 m radius are considered. It is worth noting that certain obstructed receiver locations with T-R separations of more than 200 m were detected with less than 150 dB path loss (e.g. locations near BLD, west of ENS, where diffraction above the roofs of obstructing buildings was possible).

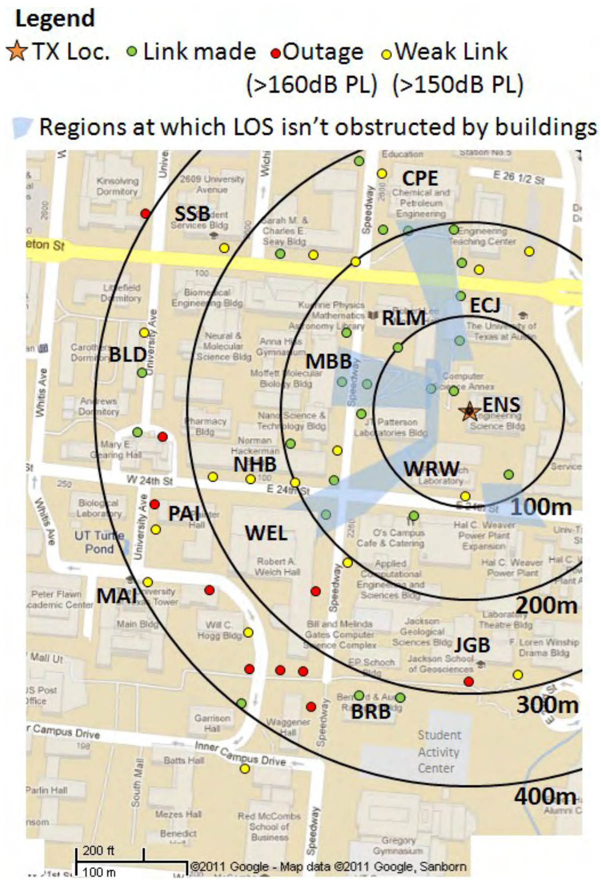

Figure 3. Outage map for ENS transmitter location (36 m high) showing receiver locations (circles) with colors corresponding to a link of less than 150 dB path loss (green), no detectable signal, i.e. outage (red), or a link of more than 150 dB but less than 160 dB path loss (yellow). Shading shows regions where there was a clear LOS view between the transmitter and the ground. An outage occurred at 18.9% of the 53 randomly selected receiver locations, while no outages were present within a 200 m radius from the transmitter.

Some obstructed links of more than 200 m also offered viable links using the transmitter on the shorter WRW building. Fig. 4 shows the WRW transmitter location and same receiver locations and measurement approach as for ENS. As expected for the lower elevation transmitter, Table I shows that links longer than 200 m were made less frequently than at the taller ENS transmitter location, resulting in an overall outage rate of 39.6% when all receiver locations are considered at 160 dB path loss. But, just as for the first transmitter location, the second transmitter location *enabled all links* (e.g. 0% outage) within a 200 m radius for a 160 dB path loss threshold. Additionally, the lower transmitter position benefited from a larger number of suitable reflectors in the environment for links under 200 m, since the vertical angle of incidence from the second transmitter location to a given reflector was reduced compared to incidence from the first transmitter location. This led to a lower number of receiver locations that had weaker but detectable links (e.g.

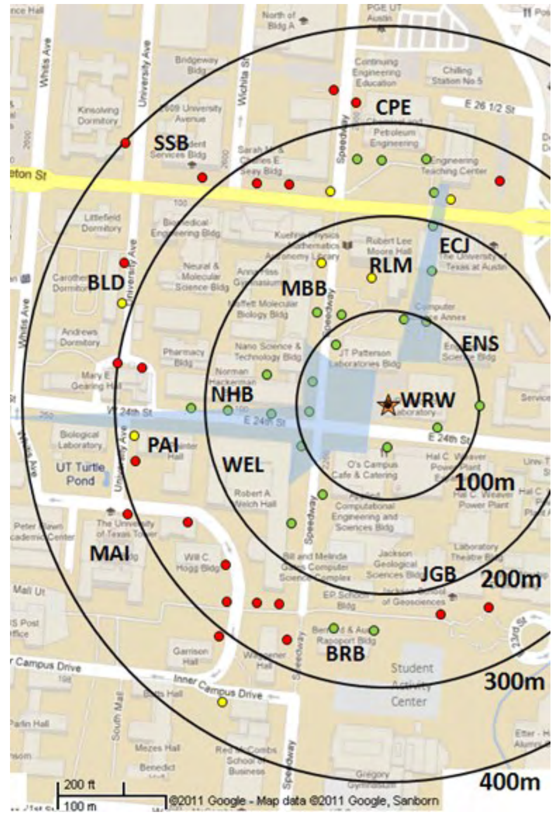

Figure 4. Outage map for WRW transmitter location (18m high). The lower transmitter height significantly reduced the number of overall links made over the 53 receiver locations, resulting in outage of 39.6%. However, like the ENS transmitter location, none of the receiver locations within a 200 m radius from the transmitter suffered an outage for 160 dB path loss.

yellow dots) with transmitter-receiver separations under 200 m when compared to the taller ENS transmitter (e.g. 6 locations were weak at WRW compared to 18 locations at ENS). For a system with a maximum detectable path loss of 150 dB, outages occurred identically at 52.8% of the receiver locations as was the case for ENS. The identical outage probability for both transmitter locations for a maximum 150 dB path loss was surprising, but can be understood by comparing Figs. 3 and 4. Note that many of the distant receiver locations at which the ENS transmitter produced links are seen as outages from the shorter WRW transmitter, while the shorter WRW transmitter location has a higher coverage rate to its nearby surroundings. This demonstrates how at mm-wave frequencies, the site-specific environment makes a very substantial "make-or-break" link due to buildings. There is little room for diffraction to "save" a link as in today's 1-2 GHz cellular systems. This clearly demonstrates the need for adaptive antennas and site-specific planning for these future mm-wave systems. Table 1 summarizes the outage probability for each transmitter location based on system sensitivity.

TABLE I. A COMPARISON OF THE OUTAGE STATISTICS FOR THE TWO TRANSMITTER LOCATIONS.

Transmitter Location	Height	% Outage for <160 dB path loss	% Outage for <150 dB path loss
TX 1 ENS	36 m	18.9% all, 0% < 200m	52.8% all, 27.3% < 200m
TX 2 WRW	18 m	39.6% all, 0% < 200m	52.8% all, 10% < 200m

Links in this work were established through both diffraction and reflection. Diffraction occurs when a signal impinges on an object that does not completely obstruct the signal's Fresnel zones [17], allowing the signal to bend around the object. Reflection occurs when a signal impinges on a very large surface that completely blocks the signal. Instead of bending around the object as in diffraction, a reflected signal will bounce off the object according to Snell's law [17] (i.e. specular reflection). The use of directional antennas at both the transmitter and receiver allowed us to record the direction from which the signal was transmitted and where it arrived from at the receiver. From the orientation of the antennas, we found that the strongest diffraction paths occurred around vertical building edges, especially when only small angles were involved. Diffraction also occurred around horizontal roof edges, e.g. when radiation from the roof-mounted transmitter was diffracted around the edge of the roof of a shorter building. Diffraction over roof edges occurred repeatedly for the tall ENS transmitter due to its 36m height.

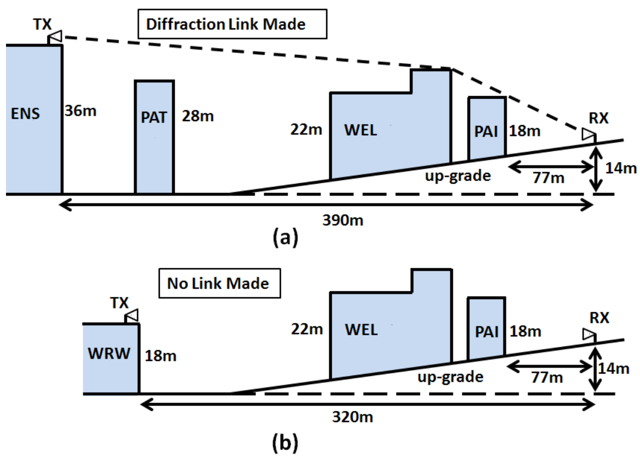

Figure 5. An example of how diffraction allows for long distance obstructed links to be created for tall transmitter locations. The receiver location next to MAI Building received a measurable signal from the ENS transmitter (36m high), but not from the lower WRW transmitter (18m high). Incline is approximated with a linear upward grade to the receiver location elevation that is 14 m higher than the transmitter building ground level elevation.

Fig. 5a visualizes one such occurrence of roof diffraction for the receiver location next to the MAI Building at the southwestern edge of the campus measurement area. With the transmitter located on ENS, a link was successfully made by diffracting over the lower WEL and PAI Buildings along the 360 m path, even though three buildings stood between the receiver and transmitter. On the other hand, this link was not established at the lower second transmitter location WRW due to WEL being taller than the WRW transmitter, as seen in Fig. 5b. Diffraction over building roofs largely explains the lower outage probability for the higher ENS transmitter, and is the reason why many distant links, such as those near the BLD Building, were able to be made.

While diffraction is common and sometimes the only mechanism for receiving a signal at an obstructed location, most links were created through reflections from buildings in the environment. Indeed, strong links were observed at several locations through reflection, when diffraction yielded a very faint signal or none at all. For instance, when the ENS transmitter was used to make a link to the receiver located in an area obstructed by RLM Building (which is 4 stories taller than ENS), a diffraction path around the corner of RLM provided a measureable multipath signal power of -80 dBm. However, once the transmitter and receiver antennas were rotated toward the cement-walled MBB Building (to the west of ENS) a reflected signal of -63 dBm was measured. In this particular situation, a 17 dB difference in path loss between diffraction and reflection was observed. The same phenomenon was observed when the transmitter was located on the roof of the WRW Building. Fig. 4 shows how three receiver locations south of the CPE building (north end of the map) at a separation distance of around 260 meters all resulted in strong links. For all three locations, the receiver and transmitter antennas were pointed in the direction of the brick-walled ECJ building. The image in Fig. 6 represents the signal path as seen from the rooftop transmitter at the top of WRW, following the orange and then green arrows as the signal is reflected off ECJ. The reflectivity of cement and brick buildings at 38 GHz can easily be predicted using site-specific methods [17],[18],[19] to accurately determine suitable base station locations, to design cells, and to analyze interference in mm-wave wireless systems.

Figure 6. In many cases when the receiver location was obstructed, reflections provided much greatrer received power than diffraction paths. A typical example involves the link produced from WRW transmitter to three receiver locations south of CPE Building from a reflection off the brick-walled ECJ Building (pictured). The arrows represent the signal path.

Notably, outages beyond 200 m were clustered for the tall ENS transmitter. For example, Fig. 3 shows that while most receiver locations near the PAI and WEL Buildings suffered outages, those near BRB and BLD Buildings provided strong links. In contrast, links over long distances for the shorter WRW transmitter showed more generalized outages, as indicated by the lower number of yellow-labeled receiver locations in the 200 m to 300 m radius range. The dependence of diffraction, reflection, and the outage clustering phenomena on the transmitter location clearly shows the value of site-specific planning and directional antennas for future millimeter-wave cellular systems. Penetration into buildings in urban cores will present challenges that warrant study.

V. CONCLUSION

We have presented a study of outage characteristics for the millimeter-wave outdoor cellular channel at 38 GHz using two different transmitter locations and 53 blindly chosen receiver locations. We found that the lower transmitter location provided better coverage over shorter distances, while the higher transmitter location had a greater coverage range. We found that obstructed links benefited frequently from reflection and diffraction paths which enabled surprisingly low outage percentages, with reflection offering 17 dB or more strength than diffracted paths. The higher transmitter location experienced fewer outages at distances over 200 m due to the signal's diffraction around lower buildings in the environment. The results of our study, which are summarized in Fig. 3 and 4 and Table 1, demonstrate that using reasonable power levels and directional antennas at the base station and mobile, no outages occurred within 200 m. This work demonstrates the potential for millimeter-wave cellular deployments, especially if site-specific planning is used to improve coverage and interference planning as part of the deployment. The channel sounding system is available for future use at New York University.

ACKNOWLEDGMENTS

This project is sponsored by Samsung Telecommunications America, LLC, and the US Army Research Laboratory (Project W911F-08-0438). The measurements were taken under FCC Experimental License 0548-EX-PL-2010.

REFERENCES

[1] Rappaport, T.S., Murdock, J.N. Gutierrez, F., "State of the Art in 60 GHz Integrated Circuits and Systems for Wireless Communications," *Proceedings of the IEEE*, Vol. 99, no. 8, pp. 1390-1436, Aug. 2011.

[2] Papazian, P.B., Hufford, G.A., Achatz, R.J., Hoffman, R., "Study of the local multipoint distribution service radio channel," *IEEE Transactions on Broadcasting,* Vol.43, No.2, pp.175-184, June 1997.

[3] Seidel, S.Y., Arnold, H.W., "Propagation measurements at 28 GHz to investigate the performance of local multipoint distribution service (LMDS)," *IEEE Global Telecomm. Conf. (Globecom)*, Vol.1, pp.754-757, Nov. 1995.

[4] Zhang, H., Venkateswaran, S., Madhow, U., "Channel Modeling and MIMO Capacity for Outdoor Millimeter Wave Links," *IEEE Wireless Comm. and Net. Conference (WCNC),* pp.1-6, 18-21 April 2010.

[5] Ben-Dor, E., Rappaport, T.S., Qiao, Y., Lauffenburger, S.J., "Millimeter-wave 60 GHz Outdoor and Vehicle AOA Propagation Measurements using a Broadband Channel Sounder," *IEEE Global Telecomm. Conf. 2011*.

[6] Rappaport, T.S., Ben-Dor, E., Murdock, J. N., Qiao, Y., "38 GHz and 60 GHz Angle-dependent Propagation for Cellular & Peer-to-Peer Wireless Communications," to appear in *IEEE Int. Comm. Conf .(ICC) 2012*.

[7] Rappaport, T.S., Qiao, Y., Tamir, J.I., Murdock, J., Ben-Dor, E., "Cellular Broadband Millimeter Wave Propagation and Angle of Arrival for Adaptive Beam Steering Systems," to appear in *IEEE Radio Wireless Symposium (RWS) 2012.*

[8] Annamalai, A., Tellambura, C., Bhargava, V.K., "Simple and Accurate Methods for Outage Analysis in Cellular Mobile Radio Systems – A Unified Approach," *IEEE Trans. on Communications*, Vol. 49, No. 2, Feb. 2001.

[9] Palestini, V. "Evaluation of overall outage probability in cellular systems," *IEEE Vehicular Technology Conference,* Vol.2, pp.625-630, May 1989.

[10] Feurestein, M.J., K.L. Blackard, T.S. Rappaport, S. Y. Seidel, H. H. Xia, "Path Loss, Delay Spread, and Outage Models as Functions of Antenna Height for Microcellular System Design," IEEE Trans. Veh. Tech, Vol. 43, No. 3, August 1994, pp. 487-498.

[11] Yeh, Y.S., Schwartz, S. "Outage Probability in Mobile Telephony Due to Multiple Log-Normal Interferers," *IEEE Transactions on Communications,* Vol.32, No.4, pp. 380- 388, April 1984.

[12] Seidel, S., Rappaport, T.S., "Site-Specific Propagation Prediction for Wireless In-Building Personal Communication System Design," *IEEE Trans. Ant. Propagation.*, Vol. 46, No. 11, pp. 879-891, Nov. 1994.

[13] Durgin, G.D., T.S. Rappaport, H. Xu, "Measurements and Models for Radio Path Loss and Penetration in and around Homes and Trees at 5.85 GHz," *IEEE Trans. on Communications*, Vol. 46, No. 11, pp. 1484-1496, Nov. 1998.

[14] S.C. Swales, M.A. Beach, and J.P. McGeehan, "A Spectrum Efficient Cellular Base-Station Antenna Architecture," *Antennas and Propagation Society International Symposium*, vol. 2, Jul. 1992, pp. 1069-1072.

[15] Elrefaie, A.F., Shakouri, M., "Propagation Measurements at 28 GHz for Coverage Evaluation of Local Multipoint Distribution Service," *Wireless Communications Conference*, pp. 12-17, Aug. 1997.

[16] Hayn, A., Bose, R., Jakoby, R., "Multipath propagation and LOS interference studies for LMDS architecture," *Eleventh International Conference on Antennas and Propagation, 2001*, vol.2, pp.686-690, 2001.

[17] DeCruyenaere, J.P., Falconer D., "A shadowing model for prediction of coverage in fixed terrestrial wireless systems," *VTC 1999 - Fall. IEEE VTS 50th Vehicular Technology Conference,* vol.3, pp.1427-1433, 1999.

[18] T. S. Rappaport, *Wireless Communication*, 2nd ed., Ch. 4, Prentice Hall.

[19] Cox, D. C., "Delay Doppler Characteristics of Multipath Propagation at 910 MHz in a Suburban Mobile Radio Environment," *IEEE Trans. on Ant. and Prop.*, vol. Ap-20, No. 5, pp. 625-635, Sept. 1972.